HRCT and pulmonary function in children with common variable immunodeficiency

Laura van Zeggeren, Annick AJM van de Ven MD, Suzanne WJ Terheggen-Lagro MD PhD, Onno M. Mets MD, Frederik J Beek MD PhD, Joris M van Montfrans MD PhD, Pim A de Jong MD PhD

University Medical Center Utrecht and Wilhelmina Children's Hospital, Departments of Radiology, Paediatric Immunology and Infectious Diseases and Paediatric Pulmonology

Laura van Zeggeren, Radiology, lauravanzeggeren@hotmail.com

Annick AJM van de Ven, Paediatric Immunology and Infectious Diseases, a.a.j.m.vandeven@umcutrecht.nl

Suzanne WJ Terheggen-Lagro, Paediatric Pulmonology, s.terheggen@umcutrecht.nl

Onno Mets, Radiology, o.m.mets@umcutrecht.nl

Frederik J Beek, Radiology, e.beek@umcutrecht.nl

Joris M van Montfrans, Paediatric Immunology and Infectious Diseases, j.m.vanmontfrans@umcutrecht.nl

Pim A de Jong, Radiology, pimdejong@gmail.com

All correspondence to:

Pim A de Jong MD PhD

University Medical Center Utrecht

Department of Radiology, HP E.01.132

Heidelberglaan 100, 3584 CX Utrecht

Email: pimdejong@gmail.com

Word count manuscript: 3080 (reference numbers excluded)

Word count abstract: 197

Number of Tables: 4. Number of Figures: 3.

Abstract

Background: High-resolution computed tomography (HRCT) may be useful to monitor lung disease in children with common variable immunodeficiency disorders (CVID). We evaluated interobserver agreement and correlation with pulmonary function tests (PFTs) for automated quantification and visual scoring of air trapping and airway wall thickening on HRCT in paediatric CVID-patients.

Methods: In a cohort of 51 children with CVID, HRCT was analysed visually and automated for presence of air trapping and airway wall thickening. PFTs were expressed as percent predicted. Disease duration, physician-diagnosed pneumonias and antibiotics prophylaxis were recorded.

Results: Interobserver agreement for automated airway wall thickening was good with an intra-class correlation coefficient of 0.88, compared to 0.51 for visual scoring. Presence of air trapping on HRCT correlated significantly with PFTs and disease duration, but was not associated with previous pneumonias. Airway wall thickening did not correlate significantly with PFTs or disease duration and was not associated with previous pneumonias or prophylactic antibiotics use.

Conclusions: In children with CVID disorders HRCT air trapping measurements are significantly correlated with PFTs and disease duration. Quantitative air trapping is a feasible and promising technique for small airways disease quantification that may be applied to monitor (silent) disease progression in CVID.

Key words: Immunodeficiency syndrome. Paediatric respiratory diseases. Radiology.

Abbreviation list

$AT_{15th\%}$	Hounsfield units number at 15th percentile
AT_{HU-850}	Number of voxels below Hounsfield Units -850 as percentage of total number of voxels
CVID	Common variable immunodeficiency
ESID	European Society for Immunodeficiencies
FEV_1	Forced expiratory volume in one second
FVC	Forced vital capacity
HRCT	High-resolution computed tomography
HU	Hounsfield units
kVp	Kilo voltage peak
LA	Lumen area
mAs	Mili-Amperage per second
MMEF	Maximum expiratory flow between 25% and 75% of FVC
PAGID	Pan-American Group for Immunodeficiency
PFTs	Pulmonary function tests
Pi	Perimeter of the inner airway lumen
RB1	Right upper lobe apical bronchus
RV	Residual volume
WA	Wall area (cm^2)
WA%	Wall area expressed as a percentage of total airway area
$WA\%_{age}$	Wall area percentage corrected for age
WA_{BSA}	Wall area normalised to body size
$WA_{-lung\ area}$	Wall area normalised to right lung area at right upper lobe apical bronchus level
WA_{Pi10}	Wall area at perimeter of the inner airway lumen of 10-mm
√WA	Square root wall area
TLC	Total lung capacity

Introduction

Common variable immunodeficiency (CVID) is a heterogeneous immunodeficiency syndrome characterized by B cell dysfunction, resulting in hypogammaglobulinemia. Because of the low levels of immunoglobulins, CVID patients are prone to develop recurrent lower respiratory tract infections. [1,2] It has been reported that 90% of CVID patients suffer from one or more episodes of lower respiratory tract infections throughout their life [3] and structural pulmonary HRCT abnormalities are reported in up to 93% of patients. [1,2] For the prevention of irreversible airway damage, CVID patients are treated with immunoglobulin replacement therapy and antibiotics as a prophylaxis or when needed for respiratory infections. Despite adequate treatment, progression of pulmonary disease occurs in a considerable number of patients and recently an overall mortality rate of 25% at 15 years after diagnosis was reported. [4,5] Because pulmonary complications are commonly seen and therapeutic options are available, it is important to monitor the presence and progression of lung disease in CVID patients [2], which can be done clinically, with laboratory tests, cultures, pulmonary function tests (PFTs) and imaging techniques. High-resolution computed tomography (HRCT) can demonstrate disease in asymptomatic CVID patients. This is important, as disease can progress without any notable episode of pneumonia, described as 'silent progression'. [6,7] Recently a CVID related lung disease HRCT score was reported aiming to quantify the structural disease component. [2] Visual scores are however time-consuming and associated with interobserver variation. Especially for visual airway wall thickening scores the interobserver variation was substantial (intra class correlation coefficient 0.51). Validated software is available to quantify airway wall dimensions [8,9] and software initially developed for emphysema quantification [10-12] could be used to quantify end-expiratory air trapping.

The aims of the current study were to evaluate the relationship of visual scores and quantitative measures of HRCT-diagnosed air trapping and airway wall thickening with PFTs in a cohort of children with CVID(-like) disease, and to determine whether observer agreement for airway wall measurements can be improved by using automated quantitative techniques.

Material and methods

Study population

Children with clinically important humoral immunodeficiencies undergo structured follow-up at our outpatient paediatric clinic. Follow-up includes a pulmonary evaluation with HRCT and PFTs. We evaluated 54 children with CVID(-like) disease who are all treated with immunoglobulin replacement therapy and showed significant clinical improvement after initiation of therapy. Because the raw HRCT data were not stored properly in one and software failed in two, three patients were excluded and the study population consisted of 51 children. These 51 HRCT scans were performed between June 2008 and June 2009; all were obtained in clinically stable patients, otherwise the scan was postponed. Thirty-three children (65%) were diagnosed with CVID according to the European Society for Immunodeficiencies (ESID)/Pan-American Group for Immunodeficiency (PAGID) [13], while 18 (35%) did not meet all of the ESID criteria for CVID. These 18 patients are defined as CVID-like (symptomatic selective antibody deficiency in combination with IgA deficiency and / or IgG subclass deficiency), but show clinical and immunological phenotypes indistinguishable from CVID patients. For antibiotic prophylaxis co-trimoxazole is used per protocol. This retrospective investigation was approved by the ethical review board and informed consent was waived.

HRCT scanning protocol

Chest HRCT scanning was performed conform a dedicated low-dose volumetric protocol on a 16-detector-row CT scanner (Brilliance-16, Philips, Cleveland, Ohio). Scans were obtained in both inspiration and expiration by using a breath-hold instruction. Inspiratory scans were acquired in a caudocranial direction with a collimation of 16*0.75mm, pitch 0.9, rotation time 0.5 seconds, 90 kilo voltage peak (kVp) and milli-Amperage per second (mAs) depending on body weight (range 16-60 mAs). Expiratory scans were acquired in a caudocranial direction with a collimation of 16*0.75mm, pitch 1.2, rotation time 0.4 seconds, 90 kVp and 11 mAs. The expiratory scan was obtained at end-expiration.

HRCT measurements

In two patients the expiration HRCT scan was obtained at insufficient exhalation (visual judgement), therefore, air trapping scores and measurements are reported for 49 HRCT scans. The visual scores for airway wall thickening and air trapping have previously been reported. [2] Two blinded independent observers scored

the extent of air trapping on a scale from 0 (absent) to 5 (>80% of the volume of a lobe affected), the extent of airway wall thickening on a scale from 0 (absent) to 3 (>67% of the volume of a lobe affected) and the average and the maximum severity of severe airway wall thickening per lobe. Airway wall thickening severity was defined as mild (airway wall thickness to accompanying pulmonary artery ratio 0.33 to 0.5), moderate (airway wall thickness to artery ratio 0.5 to 1) and severe (airway wall thickness to artery ratio >1). Abnormalities were scored for each of six lobes including the lingula. The range for air trapping was 0 (absent in all lobes) to 30 (>80%involvement of all lobes). For airway wall thickening for each lobe, the most severe score (maximum 3) is added to the average score (maximum 3), and the sum is multiplied by the extent score (maximum 3). This leads to a range of 0 (no airway wall thickening) to 108 (all airways severely thickened). The HRCT scores were expressed on a 0-100% scale. Presence of ground glass opacities was recorded.

For the automated measurements validated custom software was used (EmphylxJ). [8,9,11,12] Airway wall area (WA) and lumen area (LA) dimensions were quantified for the right upper lobe apical bronchus (RB1) and the area of the right lung at this level was measured (Figure 1). The airway quantification of RB1 was done by two independent observers in order to calculate interobserver agreement. Wall area was expressed as a percentage of total airway area ($100*WA/(WA+LA) = WA\%$). As WA% is not constant with age it was corrected for age by using the formula $WA\%_{age} = WA\% + (18 - age*0.72)$. This formula was obtained from airway measurements from a previously published study. [14] WA was also normalised to body size by dividing WA by body surface area (Mosteller formula [15], WA_{BSA}) and by the right lung area ($WA_{lung\ area}$).

Next, for airway wall quantification all perpendicular airways at every 10th CT slice were measured. We obtained perimeter of the inner airway lumen (Pi) and WA. The square root WA ($\sqrt{WA}$) was plotted on the vertical axis against Pi on the horizontal axis, resulting in a linear relationship. The linear regression formula was obtained for each patient and by using this formula the WA at a Pi of 10-mm was calculated (WA_{Pi10}).

For air trapping quantification, the lung parenchyma was segmented at every 10th expiratory HRCT slice and total number of voxels and voxels below Hounsfield Units (HU) - 850 were quantified (Figure 2). This cut-off value has been previously described [16]. The number of voxels below the cut-off was expressed as a percentage of the total number of voxels (AT_{HU-850} = 100*number of voxels below HU-850 / total number of voxels). The HU value at the 15th percentile was also calculated ($AT_{15th\%}$).

Pulmonary function tests

Two children (4%) were unable to perform spirometry and 4 (8%) could not perform plethysmography. Spirometric measurements and body plethysmographic measurements were obtained according to American Thoracic Society criteria. [17,18] Spirometric measurements included forced vital capacity (FVC), forced expiratory volume in one second (FEV$_1$) and maximum expiratory flow between 25% and 75% of FVC (MMEF). Body plethysmography included residual volume (RV) and total lung capacity (TLC). Measurements are expressed as percentage of predicted values. Reference formulas from a Dutch cohort of healthy children were used. [19] Two ratios were calculated and expressed as a percentage: RV/TLC% and FEV$_1$/FVC%.

Statistical analysis

Interobserver agreement for RB1 WA%, airway wall thickening score and air trapping score [2] was evaluated by using scatter plots with a line of identity and intra-class correlation coefficients were calculated. This correlation takes account of the distance to the line of identity. An intra-class correlation above 0.8 represents good agreement. The relation between PFTs, disease duration and HRCT parameters was visualised in scatter plots and Spearman rank correlations were calculated. Unpaired samples T-tests were used to determine whether HRCT measures differed between patients who experienced physician-diagnosed pneumonias and those who had not or those who used antibiotics prophylaxis. Analyses were performed using SPSS 15.0 (SPSS Inc Chicago, Il, USA). Statistical significance was set at $P < 0.05$. Data are reported as mean ± standard deviation (SD) and (range) unless indicated otherwise.

Results

Patient characteristics and pulmonary function

Mean age of the 51 children (38 male, 13 female) at time of HRCT was 13.1 ± 3.5 (6-18) years. Mean disease duration was 6.5 ± 3.5 (0.1-13) years. 27 of the 51 children (53%) were diagnosed with one or more pneumonias before the HRCT was performed. A total number of 22 children (43%) were using regular antibiotics prophylaxis prior to the HRCT. On average, children with CVID had a preserved lung function with FEV_1 96.3 ± 12 (66.6-129.1) %. Further details are presented in Table 1.

HRCT scores and measurements

The interobserver agreement for the automated RB1 WA% measurement was good with an intra-class correlation coefficient of 0.88. The interobserver agreement for the visual scores has been previously reported and was 0.51 for airway wall thickening and 0.78 for air trapping. [2] $WA\%_{age}$ was 72.5 ± 7.4 (54.9-92.4) %. WA_{Pi10} was 4.3 ± 0.6 (3.5-6.0) mm. Ground glass opacities were present in 7 of 49 (14%) children (Table 1).

Correlation between HRCT, PFTs, disease duration and antibiotics use

Visual air trapping score correlated significantly with FVC, FEV_1, MMEF, RV/TLC% and FEV_1/FVC(%), but not with RV/TLC% and disease duration (Table 2 and 3). AT_{HU-850} correlated significantly with MMEF and when patients with ground glass attenuation on HRCT (n = 7, 14%) were excluded this correlation became stronger and also significant for AT_{15th} (Table 2). Disease duration was also significantly associated with quantitative air trapping measures (Table and Figure 3).

For airway wall thickening, neither visual scoring nor automated quantitative measures were associated with decreased pulmonary function (Table 2) or longer disease duration (Table 3). Of note, the significant correlations of FEV_1, MMEF and RV/TLC% with quantitative airway measurements were in the opposite direction, i.e. a worse lung function was associated with a lower wall thickness. HRCT measures did not differ between patients who experienced physician-diagnosed pneumonias and those who had not or those who used antibiotics prophylaxis (Table 4).

Discussion

Airway disease is an important complication of CVID and for its monitoring HRCT and PFTs are gaining important complementary roles. We showed that in children with CVID disorders, HRCT air trapping measurements are significantly correlated with PFTs and disease duration, and that interobserver agreement for HRCT airway wall thickening assessment can be improved by using automated quantitative techniques compared to visual scores. Automated quantitative HRCT, especially for air trapping, may thus prove useful for monitoring disease progression in CVID patients.

For air trapping, we demonstrate that visual as well as quantitative HRCT measurements correlate significantly with PFTs and disease duration. For visual scoring of air trapping, other investigators [20] also found a significant correlation with PFTs in CVID patients. These and our data indicate that HRCT-diagnosed air trapping is related to relevant airway obstruction in these patients. The advantage of our study is the use of quantitative techniques of air trapping that have not previously been employed in CVID. Using this technique we demonstrate that the presence of air trapping correlates strongest with MMEF, a functional measure of small airways disease. Literature [21] suggests that airway disease in CVID, as in other diseases such as cystic fibrosis, may start in the small airways. It is likely, although we have no pathological verification, that quantitative air trapping is a sign of small airway disease that occurs already in childhood and increases with longer duration of the disease. The correlations with PFTs are stronger for visual air trapping scores than for quantitative measures. Several reasons could account for this. First, the presence of ground glass apparently had an effect on the quantitative measurements. It may be that more sophisticated air trapping measures that combine inspiratory and expiratory CT such as the relative volume change can be used to overcome this problem. [22] Second, also, differences in depth of expiration introduces noise; possibly, human observers detect an air trapping pattern at a variety of expiration levels while computerised analysis is more dependent on a stable expiration between patients. For that purpose spirometer gating or more sophisticated quantification techniques might be advantageous. [23,24] On the other hand, quantitative air trapping measurements correlated stronger with disease duration than the visual scores. Based on these results, we can neither advocate visual nor quantitative HRCT air trapping measurements for disease assessment in CVID, although the quantitative measurements have the advantage of being fully automated.

For airway wall thickening, we show neither visual nor quantitative airway wall measurements to correlate with pulmonary function or disease duration, although this does not necessarily exclude the possibility of monitoring disease progression. Quantitative airway wall measurements had not previously been employed in

9

CVID. We tried several strategies to 'normalise' the airway dimensions by age, body size and lung size for RB1 and we calculated WA at a lumen perimeter of 10-mm for all perpendicular airways as a normalisation. Nevertheless, we were unable to demonstrate a significant correlation with lung function or disease duration and can therefore not recommend a specific automated measurement or calculation of airway wall thickening. We also could not explain this lack of correlation by use of prophylactic co-trimoxazole in some patients. Others [25] have reported a significant correlation between airway wall thickening and pulmonary function in CVID, and it is generally accepted that recurrent pulmonary infections and inflammation typically cause bronchial wall thickening. An explanation for the discrepancy with our results might be that we performed HRCT in clinically stable patients, while in most other CVID studies HRCT scans are performed for a clinical indication. It may also be that in children with CVID mainly peripheral airway walls are involved. With routine CT technology these airways cannot be directly visualised and for visible airways the quantification is most accurate in airways with a diameter >2-mm as airway wall dimensions are overestimated in smaller visible airways with most software. It may well be that the airway walls of larger airways that we could quantify in our study are spared in stable CVID children. We have no clear explanation for the significant correlations of FEV_1, MMEF and RV/TLC% with quantitative airway wall measurements in the unexpected direction, and we were unable to identify any CVID-specific pathological studies of airway abnormalities that could clarify this result. In conclusion, although large airway wall thickening appears to be an acute disease marker in CVID, it appears not a good disease marker in stable children with CVID where probably airway wall disease is limited to the small airways, although it can not be excluded that longitudinal studies of airway wall thickening will be able to detect disease progression in large airway walls of stable CVID children.

We evaluated the reproducibility of HRCT measurements of air trapping and airway wall thickening. Previously [2] we described that air trapping and airway wall thickening are common findings on visually judged HRCT-scans of in CVID patients, though especially for airway wall thickening interobserver variation was considerable. Here we show that quantitative, automated measurements of airway wall thickness substantially improve interobserver agreement. We also demonstrate that fully automated quantification of air trapping (without interobserver variation) is possible and can be achieved by using a simple cut-off at HU-850 or by assessing the HU-value at the 15th percentile on the expiratory HRCT. This gain in interobserver agreement by using quantitative techniques is promising for the long-term monitoring of airway abnormalities in patients with CVID. It has been shown that quantitative airway wall measurements in other diseases such as cystic fibrosis can detect disease progression [26], and it is plausible that longitudinal studies could prove HRCT to be able to

detect (silent) disease progression in CVID patients as well, and eventually may improve clinical management in these patients.

In the present study we did not quantify bronchiectasis, which would be another interesting disease measure in these children, as bronchiectasis already occur in childhood [2]. For quantification of bronchiectasis lumen area must however be normalised by using the area of the accompanying pulmonary artery (ratio of airway lumen area to pulmonary artery area). To our knowledge no commercially available software exists for pulmonary artery area measurements. Another possibility for bronchiectasis quantification is the measurement of airway lumen tapering, but for such measurements 3-dimensional software is required.

Our study has some limitations. First, given our cross-sectional study design we can not determine whether HRCT can detect (silent) disease progression in patients with stable PFTs and absence of symptoms. As longitudinal studies are required to assess this relation, we plan to re-evaluate our cohort after two years. Second, although inadequate expiration may affect HRCT measurements, we did not control the level of inspiration and expiration by e.g. spirometry gated HRCT. Nevertheless, since we aim for a clinically applicable test and spirometer-gated scanning is not widely available, its absence strengthens the generalisability of our results. Third, no pathological correlate was available for our HRCT measurements and to our knowledge CVID-specific pathology studies of airway abnormalities have not been published. Fourth, we could not find a significant difference in HRCT measures between children who had and those who had not experienced a physician-diagnosed pneumonia. This may be due to the retrospective evaluation of these pneumonias from the patient files, leading to pneumonias that were not recorded in our study for several children. Finally, our study lacks control HRCT scans of 'healthy' children and therefore, we are unable to determine a specific cut-off level for pathology. However, at this stage our choice for quantitative or visual HRCT analysis for future research would be based on interobserver agreement and correlation with lung function.

In conclusion, we here report that automated quantitative HRCT measurements improve interobserver agreement for airway wall measurements compared to visual scores in a cohort of paediatric CVID patients. Whether wall measurements in larger airways will prove useful in stable CVID children is questionable as these measurements are not significantly associated with PFTs, disease duration or number of pneumonias. On the other hand our study can not exclude that quantitative airway wall measurements can detect disease progression or acute disease changes. Our quantitative air trapping data suggest that in stable children with CVID mainly the walls of small airways are involved and quantitative air trapping is a feasible and promising technique for small airways disease quantification that may be applied to monitor (silent) disease progression in CVID as early

11

detection of complications is of crucial importance to prevent long term morbidity, especially in paediatric

patients.

References

1. Touw CM, van de Ven AA, de Jong PA, Terheggen-Lagro S, Beek E, Sanders EA, van Montfrans JM. Detection of pulmonary complications in common variable immunodeficiency. *Pediatr Allergy Immunol*. 2010 Aug;21(5):793-805.

2. van de Ven AA, van Montfrans JM, Terheggen-Lagro SW, Beek FJ, Hoytema van Konijnenburg DP, Kessels OA, de Jong PA. A CT scan score for the assessment of lung disease in children with common variable immunodeficiency disorders. *Chest*. 2010 Aug;138(2):371-9.

3. Martínez García MA, de Rojas MD, Nauffal Manzur MD, Muñoz Pamplona MP, Compte Torrero L, Macián V, Perpiñá Tordera M. Respiratory disorders in common variable immunodeficiency. *Respir Med*. 2001 Mar;95(3):191-5.

4. Chapel H, Lucas M, Lee M, Bjorkander J, Webster D, Grimbacher B, Fieschi C, Thon V, Abedi MR, Hammarstrom L. Common variable immunodeficiency disorders: division into distinct clinical phenotypes. *Blood*. 2008 Jul 15;112(2):277-86.

5. Healy MJ. Hypogammaglobulinaemia in the United Kingdom. XII. Statistical analyses: prevalence, mortality and effects of treatment. *Spec Rep Ser Med Res Counc (GB)*. 1971;310:115-23.

6. Kainulainen L, Varpula M, Liippo K, Svedström E, Nikoskelainen J, Ruuskanen O. Pulmonary abnormalities in patients with primary hypogammaglobulinemia. *J Allergy Clin Immunol*. 1999 Nov;104(5):1031-6.

7. Plebani A, Soresina A, Rondelli R, Amato GM, Azzari C, Cardinale F, Cazzola G, Consolini R, De Mattia D, Dell'Erba G, Duse M, Fiorini M, Martino S, Martire B, Masi M, Monafo V, Moschese V, Notarangelo LD, Orlandi P, Panei P, Pession A, Pietrogrande MC, Pignata C, Quinti I, Ragno V, Rossi P, Sciotto A, Stabile A; Italian Pediatric Group for XLA-AIEOP. Clinical, immunological, and molecular analysis in a large cohort of patients with X-linked agammaglobulinemia: an Italian multicenter study. *Clin Immunol*. 2002 Sep;104(3):221-30.

8. Nakano Y, Muro S, Sakai H, Hirai T, Chin K, Tsukino M, Nishimura K, Itoh H, Paré PD, Hogg JC, Mishima M. Computed tomographic measurements of airway dimensions and emphysema in smokers. Correlation with lung function. *Am J Respir Crit Care Med*. 2000 Sep;162(3 Pt 1):1102-8.

9. Nakano Y, Whittall KP, Kalloger SE, Coxson HO, Flint J, Pare PD, English JC. Development and Validation of Human Airway Analysis Algorithm Using Multidetector Row CT. *Proceedings of SPIE*. 2002;4683:460-9.

10. Müller NL, Staples CA, Miller RR, Abboud RT. "Density mask". An objective method to quantitate emphysema using computed tomography. *Chest*. 1988 Oct;94(4):782-7.

11. Coxson HO, Mayo JR, Behzad H, Moore BJ, Verburgt LM, Staples CA, Paré PD, Hogg JC. Measurement of lung expansion with computed tomography and comparison with quantitative histology. *J Appl Physiol*. 1995 Nov;79(5):1525-30.

12. Coxson HO, Rogers RM, Whittall KP, D'yachkova Y, Paré PD, Sciurba FC, Hogg JC. A quantification of the lung surface area in emphysema using computed tomography. *Am J Respir Crit Care Med*. 1999 Mar;159(3):851-6.

13. Conley ME, Notarangelo LD, Etzioni A. Diagnostic criteria for primary immunodeficiencies. Representing PAGID (Pan-American Group for Immunodeficiency) and ESID (European Society for Immunodeficiencies). *Clin Immunol*. 1999 Dec;93(3):190-7.

14. de Jong PA, Long FR, Wong JC, Merkus PJ, Tiddens HA, Hogg JC, Coxson HO. Computed tomographic estimation of lung dimensions throughout the growth period. *Eur Respir J*. 2006 Feb;27(2):261-7.

15. Mosteller RD. Simplified Calculation of Body Surface Area. *N Engl J Med*. 1987; 22;317:1098 (letter)

16. Busacker A, Newell JD Jr, Keefe T, Hoffman EA, Granroth JC, Castro M, Fain S, Wenzel S. A multivariate analysis of risk factors for the air-trapping asthmatic phenotype as measured by quantitative CT analysis. *Chest*. 2009 Jan;135(1):48-56.

17. American Thoracic Society. Standardization of Spirometry, 1994 Update. Am J Respir Crit Care Med. 1995 Sep;152(3):1107-36.

18. Stocks J, Godfrey S, Beardsmore C, Bar-Yishay E, Castile R; ERS/ATS Task Force on Standards for Infant Respiratory Function Testing. European Respiratory Society/American Thoracic Society. Plethysmographic measurements of lung volume and airway resistance. ERS/ATS Task Force on Standards for Infant Respiratory Function Testing. European Respiratory Society/ American Thoracic Society. *Eur Respir J*. 2001 Feb;17(2):302-12.

19. Koopman M, Zanen P, Kruitwagen CL, van der Ent CK, Arets HG. Reference values for paediatric pulmonary function testing: The Utrecht dataset. *Respir Med*. 2010 Oct 1. [Epub ahead of print]

20. Gregersen S, Aaløkken TM, Mynarek G, Kongerud J, Aukrust P, Frøland SS, Johansen B. High resolution computed tomography and pulmonary function in common variable immunodeficiency. *Respir Med*. 2009 Jun;103(6):873-80.

21. Thickett KM, Kumararatne DS, Banerjee AK, Dudley R, Stableforth DE. Common variable immune deficiency: respiratory manifestations, pulmonary function and high-resolution CT scan findings. *QJM*. 2002 Oct;95(10):655-62.

22. Matsuoka S, Kurihara Y, Yagihashi K, Hoshino M, Watanabe N, Nakajima Y. Quantitative assessment of air trapping in chronic obstructive pulmonary disease using inspiratory and expiratory volumetric MDCT. *AJR Am J Roentgenol*. 2008 Mar;190(3):762-9.

23. Robinson TE, Leung AN, Moss RB, Blankenberg FG, al-Dabbagh H, Northway WH. Standardized high-resolution CT of the lung using a spirometer-triggered electron beam CT scanner. *AJR Am J Roentgenol*. 1999 Jun;172(6):1636-8.

24. Goris ML, Zhu HJ, Blankenberg F, Chan F, Robinson TE. An automated approach to quantitative air trapping measurements in mild cystic fibrosis. *Chest*. 2003 May;123(5):1655-63.

25. Gharagozlou M, Ebrahimi FA, Farhoudi A, Aghamohammadi A, Bemanian MH, Chavoshzadeh Z, Heidarzadeh M, Mehdizadeh M, Moin M, Movahedi M, Nabavi M, Pourpak Z, Rezaei N. Pulmonary complications in primary hypogammaglobulinemia: a survey by high resolution CT scan. *Monaldi Arch Chest Dis*. 2006 Jun;65(2):69-74.

26. de Jong PA, Nakano Y, Hop WC, Long FR, Coxson HO, Paré PD, Tiddens HA. Changes in airway dimensions on computed tomography scans of children with cystic fibrosis. *Am J Respir Crit Care Med*. 2005 Jul 15;172(2):218-24.

Table 1. Patient Characteristics

Characteristic	Mean ± SD or Number (%)
Total number of patients	51
Age (years)	13.1 ± 3.5
Male sex	38 (75%)
CVID	33 (65%)
CVID like disease	18 (35%)
Disease duration (years)	6.5 ± 3.5
One or more physician diagnosed pneumonia before HRCT	27 (53%)
Antibiotics prophylaxis	22 (43%)
Body surface area (m²)	1.4 ± 0.3
FEV_1 (% of predicted)	96.3 ± 12
FVC (% of predicted)	94.6 ± 11
MMEF (% of predicted)	100.8 ± 28.9
FEV_1/FVC (%)	90 ± 6.8
RV/TLC (%)	22.7 ± 6.8
Visual HRCT scores	
Air trapping present	43 (84%)
Air way wall thickening present	31 (61%)
Ground glass attenuation present	7 (14%)
Quantitative HRCT measurements	
Wall area (mm²)	24 ± 12
Wall area percentage (%)	69 ± 7.2
WA_{BSA} (mm²/m²)	18 ± 12
$WA_{lung\ area}$ (mm²/voxels)	$0.85*10^{-5} \pm 0.413*10^{-5}$
$WA\%_{age}$ (%)	72.5 ± 7.4
Measured airways at 10 mm (n)	87 ± 28.5
Wall area at Pi 10 mm (mm²)	43 ± 6
AT_{HU-850} (%)	9.3 ± 7.7
AT_{15th} (HU)	- 803 ± 53
AT_{HU-850} corrected for ground glass (%)	9.2 ± 7.7
AT_{15th} corrected for ground glass (HU)	-803 ± 53

FEV_1 = forced expiratory volume in 1 second; FVC = forced vital capacity; MMEF = maximum mid expiratory flow at 25-75% of FVC; RV = residual volume; TLC = total lung capacity; WA_{BSA} = wall area normalised to body size; $WA_{lung\ area}$ = wall area normalised to right lung area at right upper lobe apical bronchus level; $WA\%_{age}$ = wall area percentage corrected for age; HU = Hounsfield units; AT_{HU-850} = number of voxels below HU -850 as percentage of total number of voxels; AT_{15th} = Hounsfield units number at 15th percentile.

Table 2. Correlation between HRCT airway wall thickening, HRCT air trapping and pulmonary function

HRCT variables	Pulmonary function tests				
	FVC (pp)	FEV$_1$ (pp)	MMEF (pp)	FEV$_1$/FVC (%)	RV/TLC (%)
	ρ	ρ	ρ	ρ	ρ
Air trapping					
Visual score	-0.446*	-0.639*	-0.404*	-0.356*	0.293
AT$_{HU-850}$	-0.034	-0.197	-0.310*	-0.257	0.146
AT$_{15th}$	0.030	0.153	0.255	0.203	-0.176
AT$_{HU-850}$ corrected for ground glass	-0.017	-0.233	-0.402*	-0.297	0.078
AT$_{15th}$ corrected for ground glass	0.018	0.183	0.333*	0.213	-0.114
Airway wall thickening					
Visual score	-0.077	-0.113	-0.67	-0.33	0.112
Wall area	0.178	0.257	0.088	0.002	-0.396**
Wall area percentage	-0.29	-0.04	-0.032	0.043	0.124
WA$_{BSA}$	0.217	0.369**	0.343**	0.160	-0.162
WA$_{lung area}$	0.157	0.214	0.109	0.022	-0.318**
WA%$_{age}$	-0.10	0.077	0.132	0.159	0.180
Wall area at Pi 10 mm	0.11	0.07	-0.18	-0.06	-0.11

pp = percent predicted; FVC = forced vital capacity; FEV$_1$ = forced expiratory volume in 1 second; MMEF = maximum mid expiratory flow at 25-75% of FVC; RV = residual volume; TLC = total lung capacity; HU = Hounsfield units; AT$_{HU-850}$ = number of voxels below HU-850 as percentage of total number of voxels; AT$_{15th}$ = Hounsfield units number at 15th percentile; WA$_{BSA}$ = wall area normalised to body size; WA$_{lung area}$ = wall area normalised to right lung area at right upper lobe apical bronchus level; WA%$_{age}$ = wall area percentage corrected for age. Data given are Spearman rank correlation coefficients.

* Significant correlation in expected direction
** Significant correlation in opposite direction

Table 3. Correlation between disease duration, HRCT airway wall thickening and HRCT air trapping

HRCT variables	Disease duration	
	P	*P* Value
Visual score air trapping	-0.061	0.676
Visual score airway wall thickening	0.089	0.536
Wall area percentage	-0.061	0.671
WA_{BSA}	-0.038	0.797
$WA\%_{age}$	-0.274	0.052
AT_{HU-850}	0.417	0.004
AT_{15th}	-0.382	0.008

WA_{BSA} = wall area normalised to body size; $WA\%_{age}$ = wall area percentage corrected for age; AT_{HU-850} = number of voxels below HU -850 as percentage of total number of voxels; HU = Hounsfield units; AT_{15th} = Hounsfield units number at 15th percentile. Data given are Spearman rank correlation coefficients.

Table 4. Physician-diagnosed pneumonias and HRCT scores

HRCT variables	Physician diagnosed pneumonia before HRCT			Antibiotics prophylaxis (co-trimoxazole per protocol)		
	Yes (n=27) Mean (± SD)	No (n=24) Mean (± SD)	*P* Value difference	Yes (n=22) Mean (± SD)	No (n=29) Mean (± SD)	*P* Value difference
Visual score air trapping	21 (± 19)	13 (± 11)	0.108	17 (± 17)	17 (± 15)	0.899
Visual score airway wall thickening	4 (± 6)	3 (± 4)	0.462	5 (± 6)	3 (± 5)	0.390
AT_{HU-850}	12 (± 12)	9 (± 8)	0.280	11 (± 8)	10 (± 11)	0.835
AT_{15th}	-814 (± 57)	-798 (±56)	0.341	-816 (± 51)	-800 (± 60)	0.335
AT_{HU-850} corrected for ground glass	12 (± 12)	10 (± 9)	0.604	11 (± 9)	11 (± 12)	0.923
AT_{15th} corrected for ground glass	-808 (± 60)	-806 (± 51)	0.932	-814 (± 53)	-802 (± 57)	0.458
Wall area	0.21 (± 0.09)	0.27 (± 0.15)	0.127	0.25 (± 0.15)	0.24 (± 0.10)	0.771
Wall area percentage	68 (± 8)	70 (± 7)	0.296	67 (± 8)	70 (± 7)	0.100
WA_{BSA}	0.15 (± 0.05)	0.20 (± 0.15)	0.183	0.20 (± 0.16)	0.16 (± 0.07)	0.216
$WA_{lung\ area}$ ($*10^{-5}$)	0.78 (± 0.37)	0.93 (± 0.45)	0.225	0.74 (± 0.27)	0.92 (± 0.47)	0.140
$WA\%_{age}$	71 (± 8)	74 (± 7)	0.297	71 (± 8)	74 (± 7)	0.216
Wall area at Pi 10 mm	0.42 (± 0.06)	0.44 (± 0.06)	0.468	0.42 (± 0.05)	0.44 (± 0.06)	0.178

AT_{HU-850} = number of voxels below HU -850 as percentage of total number of voxels; HU = Hounsfield units; AT_{15th} = Hounsfield units number at 15th percentile; WA_{BSA} = wall area normalised to body size; $WA_{lung\ area}$ = wall area normalised to right lung area at right upper lobe apical bronchus level; $WA\%_{age}$ = wall area percentage corrected for age. Difference tested with unpaired samples T-tests.
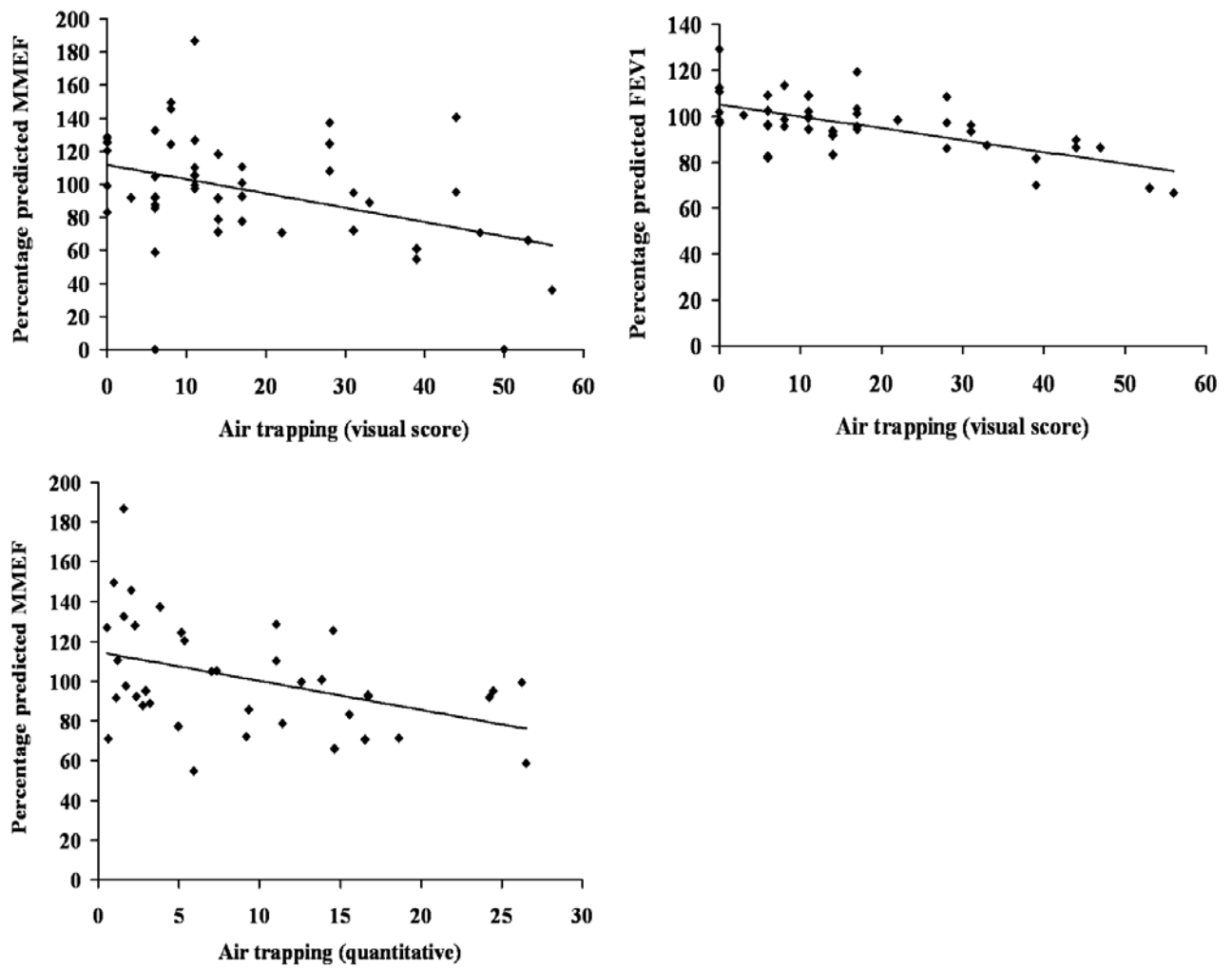
Figure 1 Airway wall quantification technique
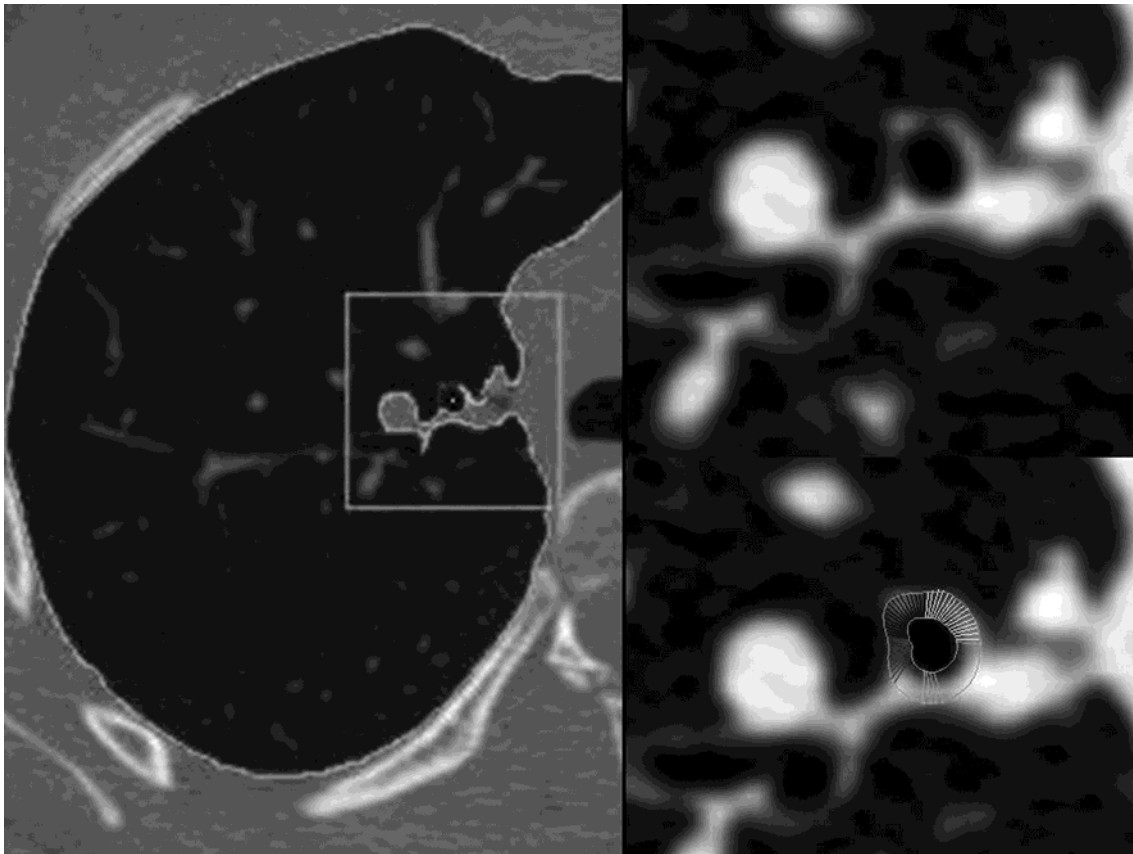
Figure 2. Air trapping quantification technique
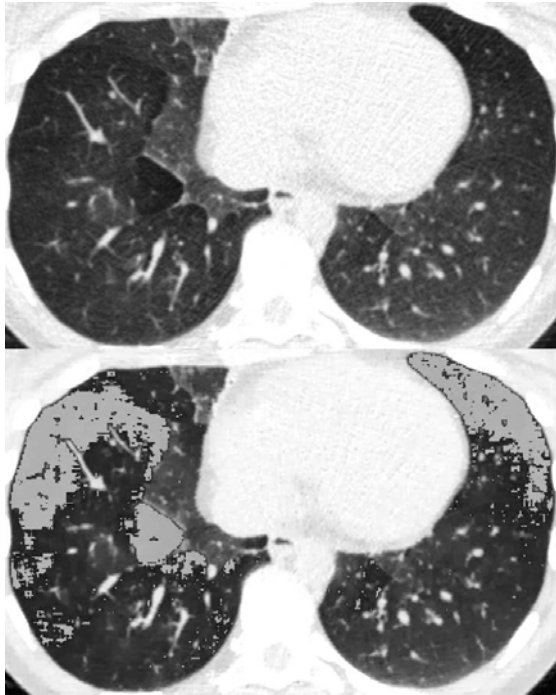
Figure 3. Correlation between HRCT air trapping and lung function

Figure legends

Figure 1: Example of automated airway measurement technique of RB1 on an inspiratory HRCT slice. RB1 is identified (left image) and selected on a detail image (right upper image). The airway wall is then automatically defined and can be adjusted manually if required (right bottom image). Right lung area at RB1 level is quantified (left image).

Figure 2: Illustration of the air trapping quantification technique on an expiratory HRCT slice. The original expiratory HRCT slice demonstrates differences in density reflecting air trapping (upper image). The voxels with a density below a certain cut-off value, in this example below HU –850, are highlighted (in grey, bottom image) and quantified.

Figure 3: Scatter plots illustrating significant correlations between visual scores for air trapping and percentage predicted MMEF (a, left upper image), and percentage predicted FEV_1 (b, right upper image), and quantitative measurements of air trapping for cut off value -850 HU in patients with no ground glass attenuation on HRCT and percentage predicted MMEF (c, bottom image). Correlation coefficients are given in Table 2.